International Journal of Nanomedicine

Dovepress
open access to scientific and medical research

Open Access Full Text Article

REVIEW

Current applications of graphene oxide in nanomedicine

This article was published in the following Dove Press journal:
International Journal of Nanomedicine
26 August 2015
Number of times this article has been viewed

Si-Ying Wu
Seong Soo A An
John Hulme

Department of Bionanotechnology, Gachon Medical Research Institute, Gachon University, Sungnamsi, Republic of Korea

Abstract: Graphene has attracted the attention of the entire scientific community due to its unique mechanical and electrochemical, electronic, biomaterial, and chemical properties. The water-soluble derivative of graphene, graphene oxide, is highly prized and continues to be intensely investigated by scientists around the world. This review seeks to provide an overview of the currents applications of graphene oxide in nanomedicine, focusing on delivery systems, tissue engineering, cancer therapies, imaging, and cytotoxicity, together with a short discussion on the difficulties and the trends for future research regarding this amazing material.

Keywords: imaging, green, cancer, therapy, diagnostics, antibacterial, cytotoxicity, contrast agent, biofunctionalization

Introduction

Graphene consists of a monoatomic layer of carbon atoms in a honeycomb lattice[1] and is one of the strongest materials ever tested with tensile strengths greater than 100 GPa and a tensile modulus of 1 TPa.[2] Biologists have shown a keen interest in this newly discovered material because of its unique chemical structure, material, and biomedical properties.[3,4] Graphene and graphene oxide (GO) sheets are easily synthesized via the Hummers method or variants thereof.[5–8] GO is hydrophilic and its surface easily modified with a host of biocompatible polymers such as chitosan,[9] polyethylene glycol (PEG),[10] poly(ε-caproplactone),[11] poly-L-lysine (PLL),[12] and polyvinylalcohol.[13] GO contains a large amount of hydrophilic groups on its edge or basal planes; thus, sheets of small size and lower concentrations should be much more biocompatible. These properties make GO extremely attractive to a large swath of scientists with new applications in the fields of drug delivery,[14–25] parasitology,[26,27] tissue engineering (TE),[28–35] antibacterials,[36–44] cancer therapy,[45–49] sensors[50–65] imaging, and diagnostics[66–75] reported monthly. To use GO in a clinical setting, it is essential to confirm its toxicity and biocompatibility through extensive in vitro and in vivo studies using specific cell lines, theoretical and animal models.[76–78] However, the safety and toxicity issue regarding GO and its potential health benefits to society are far from resolved.[79] Many previous investigations have shown GO and its hybrid structures to induce low cell toxicity, but reports remain conflicting.[80] The source of this conflict may be due to subtle epigenetic processes associated with aberrant gene expression.[81] Epigenetic mechanisms include DNA methylation at specific sites in regulatory regions such as phosphorylation, ubiquitination, and ATP-ribosylation that lead to chromatin remodeling.[81] The role of deregulated epigenetic mechanisms caused by GO and graphene-based exposure in disease pathogenesis is yet to begin.[82–84] In addition to its application in toxicity assays, functionalized GO sheets and nanoparticles (NPs) are frequently used as tissue scaffolds, fillers, and composite meshes in many areas of regenerative medicine. Studies

Correspondence: Seong Soo A An; John Hulme
Department of Bionanotechnology, Gachon Medical Research Institute, Gachon University, San 65, Sungnam 461-701, Republic of Korea
Tel +82 31 750 8755
Fax +82 31 750 8755
Email seongaan@gachon.ac.kr; flp15@gachon.ac.kr

on the relationship between stem cell differentiation and the properties of graphene derivatives are generating a tremendous impetus in the fields of cardio and neuroregeneration. GO easily combines with a host of other nanoscale materials leading to new applications in the fields of drug delivery, TE, cancer therapeutics, bioimaging, and diagnostics. This review will selectively examine the benefits and limitations of these applications and highlight the approaches that have been currently developed to clarify biocompatible and toxicity issues surrounding graphene derivatives and graphene-based hybrid biomaterials.[85–90]

Delivery systems

Drug delivery

GO and its functional derivatives exhibit an exceptional set of material properties that are frequently used to carry different therapeutics such as DNA, antibodies, proteins, genes, and small drug molecules.[91] The properties of GO relevant to drug delivery include surface area, layer number, lateral dimensions, and surface chemistry.[92] The high surface area (2,600 m^2 g^{-1}) of the single layer permits high drug loading capacity compared with other nanomaterials, but its lack of rigidity means that cell penetration is poor.[93] Lateral dimensions of GO nano-sheets do not affect drug-loading capacity but could have limitations regarding blood–brain transport, renal clearance, and biodegradation.[94] The success of a GO-based drug delivery vehicle is dependent on three factors.[78] The first is constructing a carrier with an optimal loading capacity. The second is to confirm the degree of toxicity and biocompatibility, a prerequisite prior to preclinical and clinical testing. The third is to design a system able to release drugs in a controlled manner at a designated site (tumor) for successful therapy. A common strategy to achieve efficient tumor targeting is to conjugate drug carriers with specific ligands such as polyclonal antibodies,[95] folic acid,[96] and transferrin[97] that recognize molecular signatures on the target surface.

A simpler approach to targeted drug delivery is to directly immobilize the drug onto the unmodified graphene surface. Good examples of this approach can be found in the studies by Yang et al,[98] Depan et al and Mendes et al[99,100] who showed that the anticancer molecule doxorubicin (DOX) forms a strong bond with the GO surface and that the release of DOX is more extensive in acidic or tumor environments than normal tissues. Several groups have sought to exploit the acidic environment of cancer cells by developing graphene-based vehicles containing pH-sensitive polymers. Of particular note is the work by Bai et al[102] in which a pH-sensitive GO/polyvinylalcohol hydrogel for loading and unloading the trial drug VB12 at physiological pH was developed. It was found that the percentage of drug released was dependent on the pH and salt concentration of the buffered solution. Compared with normal cells, cancer cells contain a higher level of reductive cysteine or glutathione (GSH) in their cytoplasm and endolysosomes.[102] In a recent article by Zhao et al[103] a cross-linked GO-PEG (cysteine polymethacrylic acid cross-linked nano graphene oxide polyethylene glycol) carrier possessing a novel reductive-triggering switch suited to the intracellular environment of tumor tissues was developed. The carrier released DOX six times faster at pH 5.0 in the presence of 10 mM GSH than at pH 7.4 with 10 μM GSH (stimulated normal tissues). A schematic of the fabrication process is illustrated in Figure 1. There are many other chemical strategies (esterification and biodegradation) that can be incorporated into the carrier to control the release of a drug. For example, Lu et al prepared a single layer of polyacrylic acid (PAA)-GO (1.9 nm); then it reacted with 1,3-*bis*(2-chloroethyl)-1-nitrosourea,[104] a commercial cancer drug. The multifunctional vehicle enhanced the thermal stability of the drug and significantly extended the half-life of bound 1,3-*bis*(2-chloroethyl)-1-nitrosourea from 19 to 43 hours compared with the free drug and showed efficient intracellular uptake by GL261 cancer cells. More recently Xiong et al[105] used biodegradable PEGylated NGO conjugates (nano graphene oxide disulfide linked PEG) with cleavable disulfide bonds for the photothermal therapy of A549 cells. Nano graphene oxide disulfide linked PEG showed a higher efficacy for A549 cells than the control. The drug and gene delivery applications of GO-based vehicles are summarized in Table 1.

In addition to internal cellular changes in pH, ion concentration, and temperature, there are other external methods such as ultrasound, magnetic, and electric fields than can be used to trigger the release of a drug from the carrier. A good example of external triggered release is the study by Zhou et al[106] in which a magnetic field was used to release a drug from a graphene/Fe_3O_4 nanocomposite. It was found that the weight ratio of the loaded drug to the GO carrier could reach 200%. Other examples of this concept can be found in studies by Liu et al[107] and more recently by Servant et al.[108] The latter study showed that the release of a drug from pristine graphene/methacrylic acid scaffolds could be controlled in a pulsatile fashion upon the ON/OFF application of low electrical voltages, at low graphene concentrations (0.2 mg mL^{-1}) while maintaining their structural integrity. The incorporation of highly conductive pristine graphene sheets into the

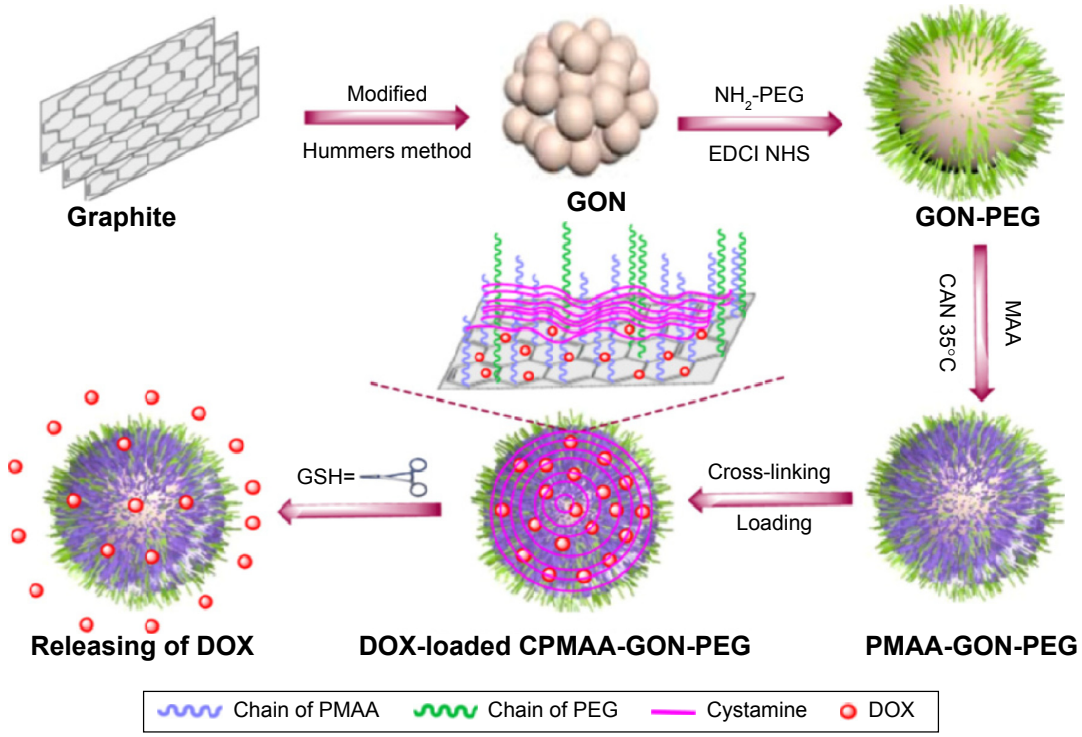

Figure 1 Schematic illustration of the preparation, ideal structural transformation, drug loading, and reduction-triggered release of the cysteine polymethacrylic acid cross-linked nano graphene oxide polyethylene glycol carriers. Reproduced with permission from Zhao X, Yang L, Li X, et al. Functionalized graphene oxide nanoparticles for cancer cell specific delivery of antitumor drug. *Bioconjug Chem*. 2015;26(1):128–136.[103] Copyright © 2015 American Chemical Society.
Abbreviations: PEG, polyethylene glycol; GSH, glutathione; DOX, doxorubicin; CPMAA, cysteine polymethacrylic acid; PMAA, polymethacrylic acid.

methacrylic-acid based hydrogel significantly decreased the resistive heat generated from the hydrogel matrix, thus minimizing necrosis to surrounding skin and tissue.

Combination therapy can be defined as the simultaneous administration of two or more active or preactive pharmacological agents that are known to disrupt multiple targets, resulting in a more efficient solution to cancer treatments. The concept of multidrug delivery was utilized by Zhang et al[27] by loading two anticancer drugs DOX and camptothecin (CPT) onto a folic acid GO carrier. The codelivery of both drugs had a better target efficacy and higher cytotoxicity than GO loaded with either DOX or CPT alone. Current chemotherapy for glioma is rarely satisfactory due to low therapeutic and efficiency and systemic side effects. A glioma-targeted drug delivery systems based on GO was recently reported[109] in which targeted peptide chlorotoxin-conjugated graphene

Table 1 Drug and gene delivery applications of GO-based vehicles

GO composite	Drug/gene	Outcome of the study	References
GO	DOX	Release pH dependent. Suited to tumor environment	98–100
GO/PVA	VB-12	pH-sensitive polymer. Suited to tumor environment	102
$CPMAA_2$-GON-PEG	DOX	The carrier showed a sixfold faster releasing rate at pH 5.0 in the presence of 10 mM glutathione	103
PAA-GO	BCNU	The multifunctional vehicle enhanced the thermal stability of the drug and significantly extended the half-life of bound BCNU from 19 to 43 hours	104
NGO-SS-PEG	DOX	NGO-SS-PEG showed a higher efficacy than NGO-PEG for antitumor therapy compared with NGO-PEG	105
Graphene/Fe_3O_4	DOX	Drugs released via magnetic or electrical stimulation	106–108
FA-GO	DOX and CPT	Codelivery of both drugs had a better target efficacy and higher cytotoxicity than GO loaded with either DOX or CPT alone	27
PPG	Adriamycin (ADR), miR-21	PPG significantly enhanced the accumulation of ADR in MCF-7/ADR-resistant cells exhibiting much higher cytotoxicity than free ADR	113

Abbreviations: $CPMAA_2$-GON-PEG, cysteine polymethacrylic acid cross-linked nano graphene oxide polyethylene glycol carrier; FA-GO, folic acid graphene oxide; GO, graphene oxide; NGO-SS-PEG, nano graphene oxide disulfide linked polyethylene glycol; PAA, polyacrylic acid; PPG, polyethylenimine poly(sodium 4-styrenesulfonate) graphene oxide; PVA, polyvinyl alcohol.

oxide sheets were loaded with DOX. Cytotoxicity experiments showed that chlorotoxin-conjugated GO/DOX mediated the highest rate of death of glioma cells compared with free DOX or GO loaded with DOX only. It is well known that codelivery is an effective treatment of cancer and other disease states.[110–112] However, multidrug resistance frequently occurs in aggressive cancers and in patients with a terminal prognosis. Recently the codelivery of novel multidrug resistance (MDR)-reversing agents and anticancer drugs to cancer cells has shown great promise as a cancer treatment. MicroRNA-21 (miR-21) overexpression is associated with the development and progression of MDR in breast cancer, and it is emerging as a novel and promising MDR-reversing target. In a recent study by Zhi et al[113] a multifunctional nanocomplex composed of polyethylenimine (PEI)/poly(sodium 4-styrenesulfonate) (PSS)/GO termed PPG was used to evaluate the reversal effects of PPG as a carrier for adriamycin (ADR) along with miR-21 targeted small-interfering RNA (siRNA) (anti-miR-21) in cancer drug resistance. Cell experiments showed that PPG significantly enhanced the accumulation of ADR in MCF-7/ADR cells (an ADR-resistant breast cancer cell line) and exhibited much higher cytotoxicity than free ADR, suggesting that PPG could effectively reverse ADR resistance of MCF-7/ADR. A schematic of the PPG fabrication process and MDR reversion is shown in Figure 2.

Gene delivery

Nonviral gene therapy is a promising approach to treat various diseases caused by genetic disorders. These carriers can transfect cells with new genes from the liquid phase in a conventionally bulky approach or from the surface of the predeposited solid phase in a substrate-mediated manner. The gene vehicle or vector must protect the loaded DNA from degradation from cellular nucleases facilitating its uptake with high transaction efficiency. The major challenge preventing the achievement of these goals is the lack of efficient and nonmutagenic vectors or gene vehicles.[114–117] Given the unpredictability of viral vectors, many researchers have turned to synthetic vectors composed of liposomes or more recently graphene derivatives. It has been shown that GO derivatives can improve the penetration of siRNA or plasmid DNA (pDNA) into cells protecting DNA from enzyme cleavage.[118] Moreover, the cytotoxicity of cationic PEI is significantly reduced after complexation or conjugation with GO.[21] In addition, Li et al[119] managed to pattern preconcentrated PEI/pDNA on absorbent GO mediating highly localized and efficient gene delivery. The patterned substrates exhibited excellent biocompatibility and enabled effective gene transfection for various cell lines including stem cells. The distinguishing property of PEI-GO compared to other vehicles is its ability to condense DNA at a low mass ratio (+49 mV)[116] and effectively transport pDNA through the cytoplasm to the nucleus. In addition, other carbon vectors such as GO/chitosan,[120] GO-PEG,[121] and GO/polyamidoamine (PAMAM)[122,123] can also be used to deliver pDNA and siRNA. Liu et al[123] showed that graphene oleate PAMAM exhibited good compatibility and greatly improved green fluorescent protein gene transfection efficiency (18.3%) in contrast to ultrasonicated graphene (1.4%) and GO PAMAM without oleic modification (7.0%).

Besides its ability to protect DNA, graphene possesses the unique optical property of absorbing near infrared (NIR) light. Tian et al[124] showed that localized NIR heating of GO-PEG-Ce6 increased its uptake and efficacy against cancer cells. They attributed the enhanced uptake of GO-PEG-Ce6 to an increase in membrane fluidity upon NIR heating. Moreover, Kim et al[125,126] demonstrated that NIR irradiation of functionalized reduced GO can change the membrane

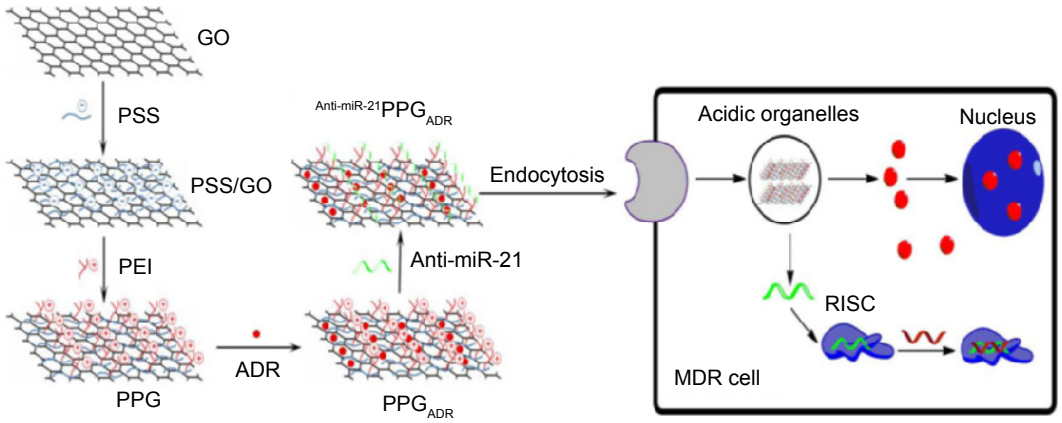

Figure 2 Fabrication of polyethylenimine poly(sodium 4-styrenesulfonate) graphene oxide delivery vehicle and MDR reversion. Reproduced from Zhi F, Dong H, Jia X, et al. Functionalized graphene oxide mediated adriamycin delivery and miR-21 gene silencing to overcome tumor multidrug resistance in vitro. *Plos One*. 2013;8(3):e60034.[113]
Abbreviations: GO, graphene oxide; PLL, poly-l-lysine; PSS, poly(sodium 4-styrenesulfonate); PEI, polyethylenimine; PPG, poly(sodium 4-styrenesulfonate) (PSS)/GO; ADR, Adriamycin.

integrity of endosomes, thus improving the intracellular lifetime of the drug or gene and their delivery efficacy.

Tissue engineering

As well as DNA, GO is also used to deliver specific proteins such as bone morphogenetic proteins (BMPs) and substance P (SP) factors.[127–129] Among BMPs, BMP-2 is a well-known growth factor used for bone regeneration. A large dose of BMP-2 leads to several side effects such as over bone growth, inflammation, and uncontrolled bone formation. In a recent study, La et al[35] demonstrated that the surface of a Ti-GO implant can be preloaded with several BMPs and SP. BMP-2 delivery using GO-Ti or GO-coated Ti exhibited a higher alkaline phosphatase activity in bone-forming cells in vitro compared with bare Ti. The dual delivery of BMP-2 and SP (a selective agent for mesenchymal cell differentiation) showed the greatest formation of bone growth in mouse calvaria compared with the other groups.

The development of highly organized and functional 3D complex scaffolds in vitro is of great importance in TE, since native tissues and organs exhibit highly organized and multifunctional architectures composed of extracellular matrix, different cell types, and chemical and physical signaling clues. Cardiomyocytes are particularly interesting forming dense quasi-lamellar and high vascularized tissue in heart muscle.[130,131] Mimicking the vascularized structures of the myocardium with various types of cell still remains one of the major challenges in TE. Some of the most commonly used methods are bottom up assembly[132] or the layer-by-layer[133,134] (LBL) approach. In a recent article by Shin et al[135] high interlayer conductivity and strong cellular adhesion was achieved in a multilayer cell construct using functional PLL-GO NPs (GONs) and the LBL approach. The 3L construct made with PLL-GO promoted thicker tissue growth (65 µm) compared with the construct without PLL-GO as a control (23 µm). The thickness and size of the layers PLL-GO layers ranged from a few microns to 10 µm, which is much thicker than tissue grown on using fibronectin, gelatin (G), and nanofilms (6.2 nm). The advantages of using PLL-GO layers can be seen in the confocal cross-sectional images of the 3L tissue constructs and the control group after 2 days of culture (Figure 3).

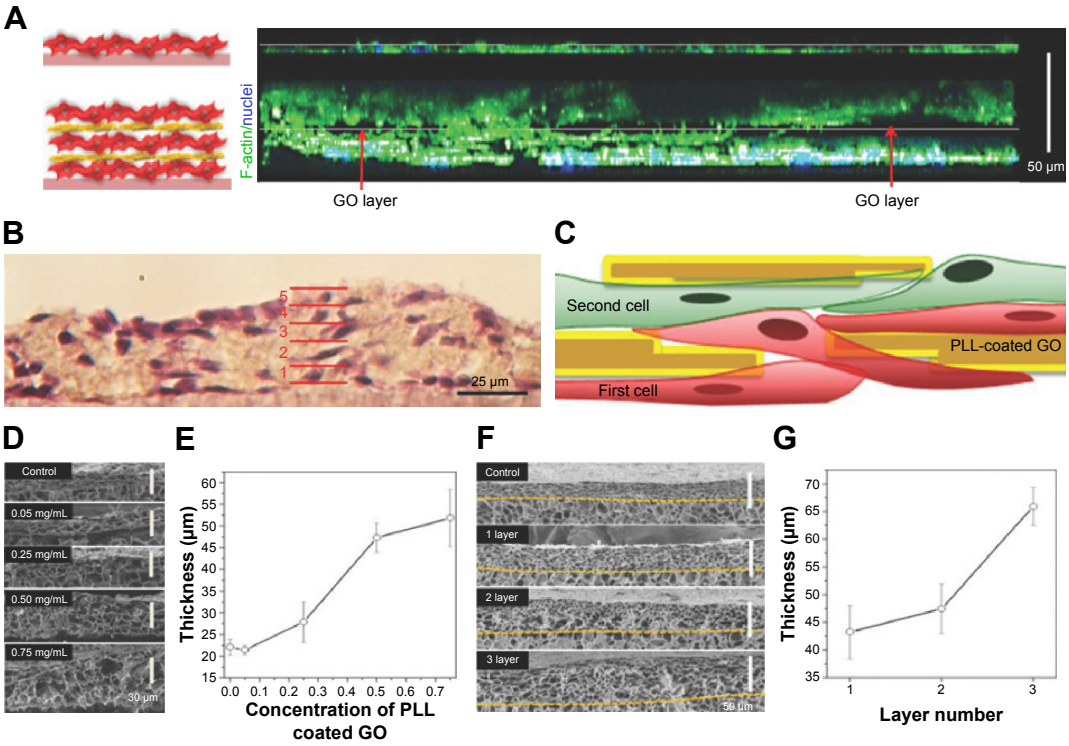

Figure 3 (**A**) Confocal cross-sectional images of the control group (top) and the 3L tissue constructs (bottom) after 2 days of culture. F-actin and cell nuclei were labeled with green and blue fluorescent dyes, respectively. The 3T3 fibroblasts were found to connect the cells on the first layer to the cells on the second layer through noncontinuous PLL-coated GO layer (red arrow, empty black area). (**B**) Hematoxylin and eosin (H&E) stain images of 3L 3T3 fibroblasts. The solid red lines indicate the interfaces between each layer. (**C**) Schematic illustration of the cross-section of the 2L construct showing the cells residing above and below the PLL-coated GO nanofilms. (**D**) SEM images showing the cross-section and (**E**) the thickness of 2L constructs fabricated with various concentrations of PLL-coated GOs as interlayer GO films. (**F**) SEM images showing the cross-section, and (**G**) the thickness of 1L, 2L, and 3L constructs. The thickness of the constructs was estimated from the corresponding SEM images. Reproduced from Shin SR, Aghaei-Ghareh-Bolagh B, Gao X, et al. Layer-by-layer assembly of 3D tissue constructs with functionalized graphene. *Adv Mater*. 2014;22(39):6136–6144.[135] Copyright © 2015 Wiley ACH.

Abbreviations: GO, graphene oxide; PLL, poly-L-lysine; SEM, scanning electron microscope.

Silk fibrin (F) proteins are routinely employed in tissue generation as substitutes for bone and skin tissues and blood vessels. Utilizing the material advantages of Fibrin and GO, Wang et al fabricated a nanocomposite film by simply casting the two components together.[138] Fibrin functionalized graphene oxide and GO can also be used as nucleation sites for the growth of hydroxyapatite (HA). Deepachitra et al[139] showed that fibrin-graphene hydroxyapatite (FGHA) was an excellent platform for osteoblast cell growth and maturation, showing very high viability rates compared with GO, GOHA, and functionalized graphene oxide. Chaudhuri et al have sought to overcome the problems of toxicity and biocompatibility by blending the insulating polymer polycaprolactone with GO nanoplatelets resulting in a highly conductive biocompatible scaffold.[138] The resulting scaffold was used to differentiate human cord blood-derived mesenchymal stem cells into skeletal muscle cells. It was concluded that the addition of GO nanoplatelets enhanced both conductivity and the dielectric constant of the GO-polycaprolactone scaffold stimulating highly oriented multinucleated myotube formation. Studies have proved the ability of GO to promote stem cell differentiation into osteogenic, cardio, neuronal, and adipogenic lineages.[140–143] Of particular note is the recent work by Kim et al[33] in which a novel strategy to guide stem cell differentiation into specific cell lineages by employing combinatorial GO hybrid-patterns of specific geometries was reported. NGO combinatorial pattern-arrays, with different sizes and geometries, were successfully transferred to various substrates such as Au-coated glass, molded polystyrene, flexible polydimethylsiloxane, and even biodegradable poly(lactic-co-glycolic acid) film. The NGO line patterns generated on both rigid gold substrates and flexible polymers were effective for guiding osteogenic differentiation of human adipose-derived mesenchymal stem cells (hADMSCs) with conversion efficiencies as high as 54.5% and 41%, respectively. In addition, patterned GO resulted in a conversion ratio of MSCs to neurons of up to 30%.The enhanced neuronal differentiation of hADMSCs via patterned NGO could result in improved treatments of serious neurological disorders such as Parkinson's disease. A schematic showing neuronal differentiation of hADMSCs using different NGO grid-patterned substrates is shown in Figure 4.

GO is also known to play a significant role both in endothelial and hepatocyte cell proliferation and morphology differentiaton. Zhou et al[136] also showed that a LBL 3D composite layer composed of PSS (polyanion) and polyacrylamide (poly-cation) grafted to GO exhibited excellent anticoagulant bioactivities indicating heparin-mimicking activity. In another LBL study,[137] assembled GO nanocomposite films were constructed aimed at improving the mechanical properties of polyelectrolyte multilayer (PEM) films containing PSS and poly(allylamine hydrochloride). It was found that a single layer of GO improved the elastic modulus of a PEM film by up to 181%.[137] When compared with native PEM films, fibroblast cells grew quicker and over a larger area, forming numerous and better organized adhesion points on the GO composite films.

Imaging techniques

In the last 10 years, a lot of effort has been dedicated in exploiting graphene derivatives as contrast agents (CAs) for intracellular imaging in vitro and in vivo. There are many examples of functionalized GO being employed as fluorescence and photoluminescent vehicles in cellular imaging. Of particular note is the recent work by Sreejith et al[144] in which a hybrid material composed of organic dyes, mesoporous silica nanoparticles (MSNPs), and GO was synthesized. Squarine dyes were loaded inside MSNPs, and the MSNP surfaces were then wrapped with ultrathin GO sheets. The hybrid was biocompatible, noncytotoxic exhibiting significant potential for in vitro fluorescence imaging as confirmed by the imaging studies with HeLa cells.

Magnetic resonance imaging (MRI) is a central whole-body imaging techniques used to visualize anatomical structures in biomedical research and clinical medicine. Researchers have been developing MRI CAs since the 1980s.[145] CAs are complexes of gadonlinium (Gd^{3+}), manganese (Mn^{2+}), or iron (Fe^{2+}). Gd^{3+} chelate-based T_1 MRI CAs currently dominate the market (have >95% market share) with nearly half of all MRI procedures in the United States using MRI CAs. However, the Food and Drug Administration recently restricted the clinical use of Gd^{3+} chelates for patients affected by renal failure. CAs using Mn^{2+} ions have been proposed as possible alternatives. Kanakia et al[146] showed that GO/Mn^{2+}/Dextran (GNP-Dex) agents performed particularly well. The results indicated that at high concentrations between 0.1 and 100.0 mg/mL, the GNP-Dex formulations were hydrophilic, stable in deioinzed water, as well as iso-osmolar (upon addition of mannitol) isoviscous to blood. At potential steady state equilibrium concentrations of blood (0.1–10.0 mg/mL), protein binding, and histamine release studies indicated that GNP-Dex formulations are thermally stable and elicit negligible allergic response. The r1 relaxivity of GNP-Dex was 92 mM^{-1} s^{-1} (per-Mn^{2+} ion, 22 MHz proton Larmor frequency); approximately 20- to 30-fold greater than that of clinical Gd^{3+}- and Mn^{2+}-based CAs.

Other examples[147] utilizing magnetize GO hybrids for imaging can be found in the study by Gollavelli et al in

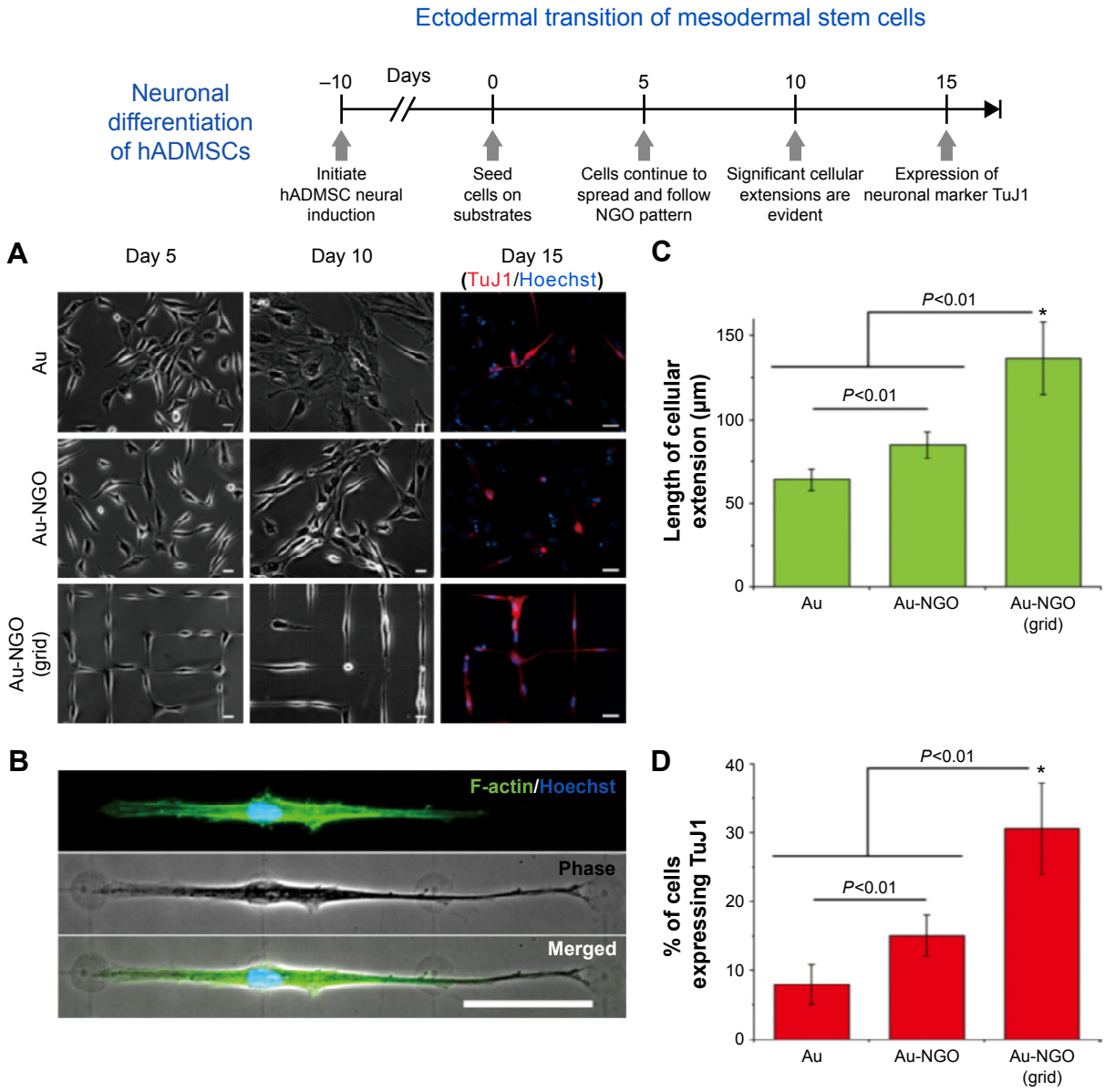

Figure 4 Neuronal differentiation of hADMSCs using NGO grid-patterned substrate.

Notes: (**A**) Images of neural-induced hADMSCs grown on poly-L-lysine-coated Au (Au), NGO-coated Au (Au-NGO), and NGO grid-patterned substrates (Au-NGO (Grid)). All substrates were coated with laminin to facilitate cell attachment. Cellular growth and morphology were monitored over 15 days, followed by staining for the neuronal marker TuJ1 (red) and nucleus (blue). Scale bars =20 μm. (**B**) Phase-contrast and fluorescence images of cells stained for F-actin (green) and nucleus (blue) after 15 days of cultivation show extensive cellular extension on NGO-grid patterns. Scale bar =50 μm. (**C**) Quantitative comparison of the length of cellular extension on various substrates (n=3; *$P<0.01$, Student's unpaired *t*-test). (**D**) Quantitative comparison of the percentage of cell expressing the neuronal marker TuJ1 on various substrates (n=3; *$P<0.01$, Student's unpaired *t*-test). Reproduced with permission from Kim TK, Shah S, Yang L. Controlling differentiation of adipose-derived stem cells using combinatorial graphene hybrid-pattern arrays. *ACS Nano*. 2015:9(4):3780–3790.[33] Copyright ©2015 American Chemical Society.

Abbreviations: NGO, nano graphene oxide; TuJ1, class III beta-tubulin.

which reduced graphene was covalently modified with a PAA bridge then linked to fluorescein *o*-methacrylate. The PAA bridge was found to inhibit both vehicle aggregation and graphene-induced fluorescence quenching of conjugated fluorescein *o*-methacrylate. Toxicological studies showed the resultant hybrid to be nontoxic with insignificant amounts of reactive oxygen species (ROS) and apoptosis in HeLa cells. Confocal laser scanning microscopy images further revealed images that the hybrid was localized in the cytoplasm at the cellular level and exhibited a broad distribution from the head to the tail in zebrafish (animal model). Considering their large surface GO sheets can also be integrated with various types of NPs to form multifunctional nanomaterials for different application purposes.

MR and X-ray computed tomography (CT) imaging modalities are widely used for various experimental and

clinical applications. MR offers high sensitivity and good discrimination particularly in soft tissue but shows no signal for high-density calculus and gland calcification. CT affords better spatial and density resolution than other modalities but is limited by the poor performance of iodine-based CAs in soft tissue. Thus, combining MR imaging with CT modality could achieve more useful information of soft tissues or tumors with enhanced accuracy. Recently, a GO-$BaGdF_5$ nanocomposites[148] for multimodal imaging was fabricated using a solvo-thermal method in the presence of PEG; $BaGdF_5$ NPs were firmly attached on the surface of GO nanosheets to form the GO/$BaGdF_5$/PEG. The composite showed low cytotoxicity, positive MR contrast effect, and better X-ray attenuation property than lohexol, which enabled effective dual-modality MR and X-ray CT imaging of a tumor model in vivo. Moreover, histological examination and serum biochemistry assay revealed no apparent toxicity of the CA to mice after treatment. GO/$BaGdF_5$/PEG may be further conjugated with different targeting ligands to construct multifunctional systems for targeted theranosis of cancers. A schematic summarizing the dual-imaging capabilities of GO/$BaGdF_5$/PEG is shown in Figure 5.

Hong et al[149] fabricated a targeted multifunctional GO hybrid via the covalent linkage of PEG, fluorescein isothiocyanate, 1,4,7-triazacyclononane-1,4,7-triacetic acid (NOTA), and TRC105 (a monoclonal antibody that binds to CD105) on GO. The pharmacokinetics and tumor-targeting efficacy of the NOTA/TRC105/GO hybrid were investigated with serial noninvasive positron emission tomography imaging and biodistribution studies, indicating excellent stability and target specificity. New preparation[150] methods were also employed in the construction and detection of graphene-based hybrids for magnetic resonance/fluorescence imaging. A magnetic Fe_3O_4-doped carbogenic nanocomposite (IOCNC) was synthesized by thermal decomposition of organic precursors in the presence of F_3O_4 NPs with a mean diameter of 6 nm. Magnetic studies confirmed the superparamagnetic behavior nature of IOCNC at room temperature. IOCNC showed MR contrast behavior by affecting the proton relaxation phenomena. The measured longitudinal ($r_1=T_1$) and transverse ($r_2=T_2/T_2$*) relaxivity values are 4.52 and 34.75 mM^{-1} s^{-1}, respectively. The hybrid showed a biocompatible nature with no apparent cytotoxicity. In vivo MR studies indicated both T_1 and T_2 contrast behaviors of the hybrid. Fluorescence imaging indicated selective uptake of IOCNC by macrophages in spleen. Pharmacokinetics and tumor targeting efficacy of the hybrid was evaluated via positron emission tomography imaging using Ga as the radiolabel. GO linked covalently with PEG was conjugated to NOTA and TRC105, making the hybrid specific toward

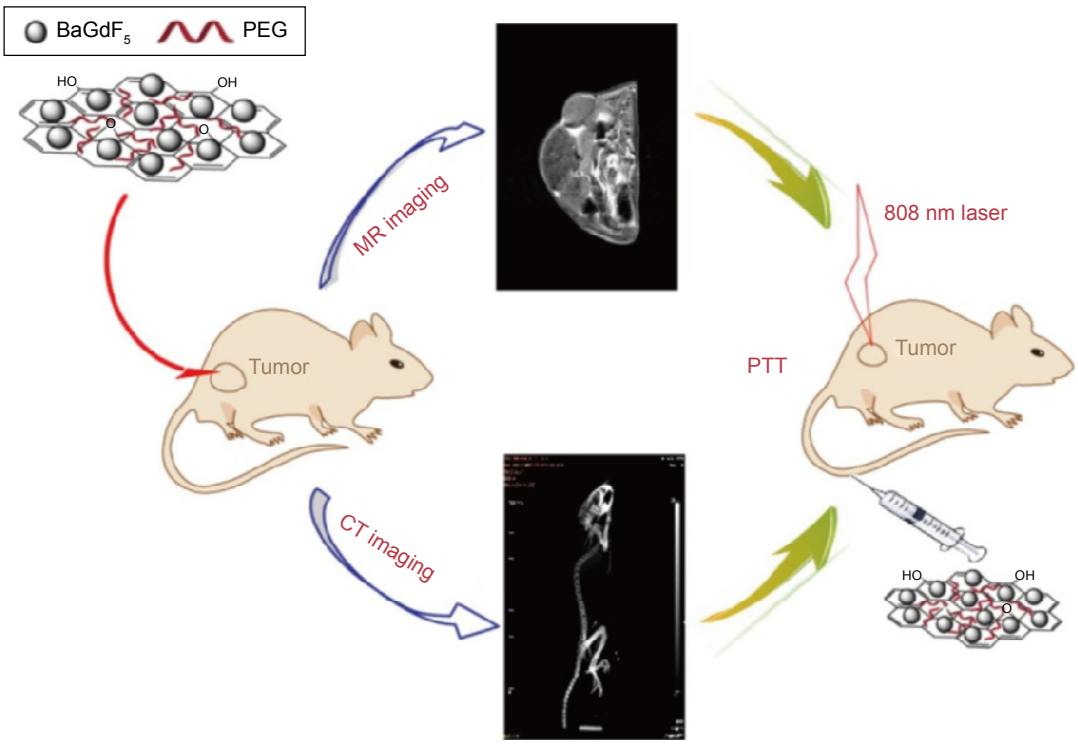

Figure 5 A schematic diagram of magnetic resonance (MR)/computed tomography (CT) imaging and near infrared photothermal therapy (PTT) using the graphene oxide/$BaGdF_5$/polyethylene glycol (PEG) nanocomposites. Reproduced with permission from Zhang H, Wu H, Wang J, et al. Graphene oxide-BaGdF5 nanocomposites for multimodal imaging and photothermal therapy. *Biomaterials.* 2015;42:66–77.[148] Copyright © 2015 Elsevier.

CD105 in cell culture. In $4T_1$ tumor-bearing mice, the Ga/NOTA/GO/TRC105 and Ga/NOTA/GO composites were primarily cleared through the hepatobiliary pathway. Ga/NOTA/GO/TRC105 was accumulated quickly in $4T_1$ tumors with uptake remaining stable up to 24 hours postinjection. In active targeting, GONs with antibody, peptide, or protein coatings can bind specifically to the surface of tumor cells or to neovascular endothelial cells. However, certain challenges remain, as shown by the limited performance of the first clinically approved PEGlyated liposome (Doxil™). In immunodeficient animal models, the liposome exhibited marked antitumor effects, but in clinical applications, liposomes exhibited efficacy against only a limited number of tumors, such as Kaposi's sarcoma. This can be attributed to the complexity of the tumor morphology during the successive stages of inflammation, fibrillization, hemorrhage, and repair that occur repeatedly in the process of tumor formation and growth in humans.[151]

Photodynamic therapies

The strong optical absorbance of graphene-based nanomaterials in the NIR region makes them generally applicable as prognostic, diagnostic, and therapeutic agents in the treatment of cancer and other disease states. Photodynamic therapy (PDT)[152] is a popular cancer therapy method that involves the delivery of photosensitizers (PS)[153] into the cancer cells generating cytotoxic ROS (photodynamic) or generating heat (photo-thermal) that are capable of killing cells through photoablation. In addition, PDT has been shown to damage tumor vasculature through direct effects on vascular endothelial cells. Ideally, PDT agents should exhibit strong absorbance. However, clinical application of PDT is limited by the hydrophobic nature and poor tumor selectivity of existing PSs.[154] 2-(1-Hexyloethyl)-2-devinyl pyropheophorbide-alpha (HPPH, Photochlor))[155–157] is a second-generation PS currently progressing through phase I/II clinical trials and has shown excellent safety and efficacy for the treatment of lung, Barett's esophageal, and head and neck cancers. GO and reduced graphene oxide (rGO) are reported to induce lung toxicity in mice when delivered orally or intravenously, but when coated with PEG and chitosan are nontoxic to cells in vitro and can be cleared via renal and hepatic routes. Recent work using HPPH loaded onto GO by Rong et al[158] showed a dramatic improvement in photodynamic cancer cell kill efficacy due to the increased tumor delivery of HPPH within the tumor compared with free HPPH upon 671-nm laser irradiation. The study highlighted the advantages of GO as a carrier for PDT resulting improvements in PDT efficacy and long-term survival rates of tumor mice following treatment.

Ultrafast laser is an effective tool for nanofabrication due to the high-pulse energy; the temperature of GO can increase by more than 1,000°C in microseconds, simultaneously reducing GO to rGO. Moreover, the ultrafast reduction of GONs with a femtosecond laser beam creates extensive microbubbling.[159] The instant collapse produces a microcavitation effect that brings about localized mechanical damage. A study by Li et al[160] showed that when microbubbles are produced the effective laser power was reduced to less than half of what is needed when microbubbling is absent. Gastric cancer cells labeled with PEG-transferrin required only a few scans of a 4 mW laser source for cell therapy, while 15 scans of a 9 mW source resulted in the death of only a few cells labeled with rGONs. This technique may be particularly useful in dealing with fibrotic intractable tumors often accounted in pancreatic cancers. A detailed review regarding the theranostic applications of graphene in cancer can be found in a recent article by Chen et al.[161]

Cytotoxicity

PEGlyated GO and GO exhibit certain advantages in vitro and in vivo drug delivery, such as high drug-loading efficiency, passive and active targeting capabilities, and reversal effects against cancer drug resistance.[93] PEGylation is known to improve the solubility of hydrophobic nanomaterials and is widely used in many areas of nanomedicine.[25] Reports have shown that incubation of several cell cultures, such as glioblastoma cell line (U87MG), breast cancer cells (MCF-7), human ovarian carcinoma cell line (OVCAR-3), colon cancer cell lines (HCT-116), and lymphoblastoid cells (RAJI) with GO-capped PEG[162–164] exhibit no cytotoxicity up to 100 μg/mL. The ability of macrophages to internalize and remove graphene materials from the site of deposition serves to enhance their cellular biocompatibility. For example, two phagocytic cell lines were able to internalize and micronized GO with different lateral sizes showing a selective internalization. After internalization, GO accumulated in the cytoplasm, perinuclear space, and nucleus of the cell.[165] Mu et al revealed that C2C12 progenitor cells used clathrin-mediated endocytosis to internalize medium-sized GO (500 nm) and phagocytosis for larger micron (1–2 μm)-sized sheets. Shortly after, both types of GO entered lysosomes for excretion. Almost no inhibition of cell proliferation was found at doses up to 100 μg/mL.[166]

The in vitro hemocompatibility and genotoxicity of GO with human primary blood components remains a hotly

contested issue. Initial studies examining the hemocompatibility of graphene and GO showed that graphene exerted a slightly higher cytotoxic effect than GO due to its strong hydrophobic interaction with cell membranes with both materials exerting insignificant hemolytic effect (up to 75 μg/mL).[167] In contrast, Liao et al[168] demonstrated that submicron-sized GO sheets induced the greatest hemolytic activity, whereas aggregated graphene sheets exhibited the lowest hemolytic activity. Coating the oxidized sheets with chitosan almost eliminated hemolytic activity. It was concluded that the toxicity of graphene and GO was dependent on the exposure environment (ie, whether or not aggregation occurs) and mode of interaction with cells (ie, suspension versus adherent cell types). In a recent investigation, Ding et al[169] examined the hemocompatibility of GO on human peripheral blood T lymphocytes and human serum albumin (HSA). In that work, the underlying toxic mechanisms of pristine GO (p-GO) and functionalized GO (GO-COOH and GO-PEI) to primary human peripheral blood T-lymphocytes and HSA were investigated. p-GO was found to interact directly with the protein receptors to inhibit their ligand-binding ability, leading to ROS-dependent apoptosis through the B-cell lymphoma-2 (Bcl-2) pathway; GO-COOH exhibited a similar degree of toxicity on T lymphocytes except keeping a normal ROS level. Ding et al proposed that GO-COOH inhibits protein-ligand binding and passes the passive apoptosis signal to nucleus DNA through a ROS-independent mechanism. GO-PEI showed severe hematotoxcity to T lymphocytes by inducing membrane damage. For HSA, the binding of GO-COOH resulted in minimal conformational change and HSA's binding capacity to bilirubin remained unaffected, while the binding of p-GO and GO-PEI exhibited strong toxicity on HSA. A schematic of the toxic mechanism of GO on T lymphocytes is depicted in Figure 6. These apparent contradictions in the literature are most probably due to poor-quality GO being used (broad lateral distributions >500 nm and the presence of contaminants, Mn^{2+}, Fe^{3+}, Cu^{2+}) and inconsistencies in assay design (MTT false positives and GO's strong autofluorescence signal). At concentrations approximate to 50 μg/mL or higher, freshly prepared GO begins to show toxicity against erythrocytes, fibroblasts, and, in some reports, PC12 cells as well. PEGylation significantly improves biocompatibility, but the chemical bonds linking GO with the surfactant can be broken releasing PEG and its derivatives into the surrounding environment. The influence of PEG to suppress heme destruction and improve peroxidase function was recently reported by Mao et al.[170] It was found that horseradish peroxidase (HRP) inactivation is significantly mitigated in the presence of PEG. In addition, recent reports show that the concentration of HRP oligomers produced from the biocatalysis of GO was undetectable.[171] It is well reported that carbon nanotubes are rapidly degraded by HRP, myeloperoxidase, eosinophil peroxidase with HRP-catalyzed oxidation of single walled carbon nanotubes and GO (single-walled carbon nanotubes) reported to induce DNA damage.[172] Whether the localized release of PEG from

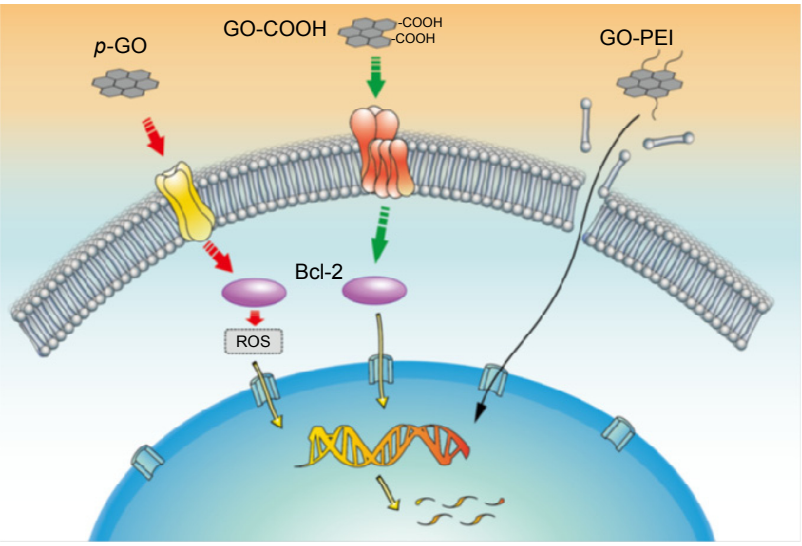

Figure 6 Schematic diagram showing proposed toxic mechanisms of GO on T lymphocytes based on the current data. From left to right are p-GO, GO-COOH, and GO-PEI, respectively. Dotted line indicates signal pathway, and full line indicates the way of GO-PEI transport. Reproduced with permission from Ding Z, Zhang Z, Ma H, Chen Y. In vitro hemocompatibility and toxic mechanism of graphene oxide on human peripheral blood T lymphocytes and serum albumin. *ACS Appl Mater Interfaces*. 2014;6(22):19797–19807.[169] Copyright ©2015 American Chemical Society.
Abbreviations: Bcl-2, B-cell lymphoma-2; PEI, polyethylenimine; p-GO, pristine graphene oxide; ROS, reactive oxygen species.

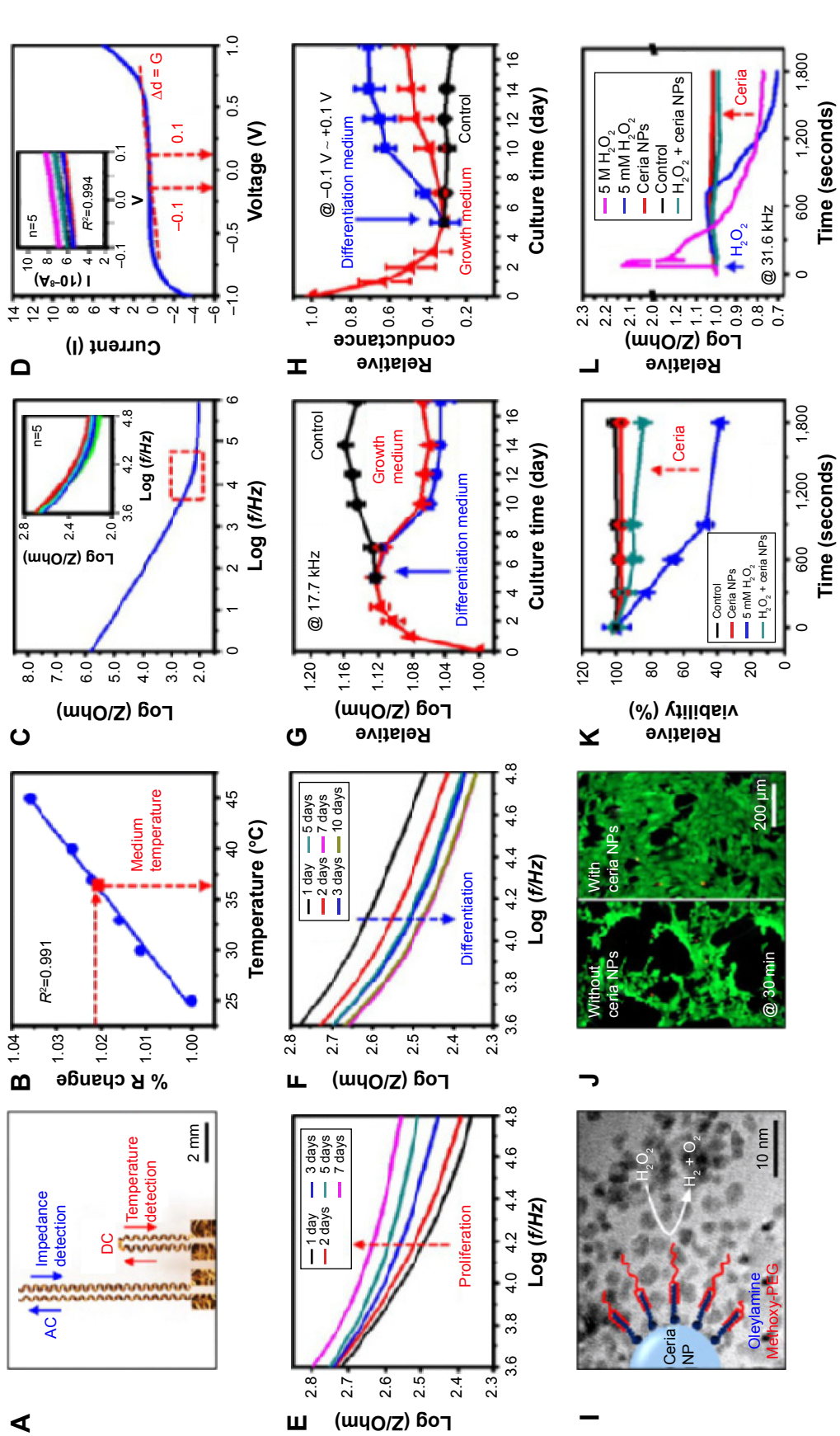

Figure 7 Physiological monitoring of C2C12 myoblasts by impedance/temperature sensors and in vitro tests of the efficacy of ROS scavenging nanoparticles.

Notes: (**A**) Impedance and temperature sensors integrated on a PDMS substrate. (**B**) Calibration curve of temperature sensor: normalized resistance (% R change) as a function of temperature. The red arrow indicates the temperature of the growth medium during the culture. (**C**) Electrical characterization of the impedance sensor in the growth medium at 37°C. Impedance curve measured from 1 Hz to 1 MHz with a bias voltage of 0.01 V. The inset shows the magnified view of the red-dotted region. Repeated measurements show minor deviations. (**D**) Current-voltage (*I–V*) curve, whose slope indicates the conductance. The inset shows the magnified view. Repeated measurements confirm the stability of the sensor. (**E** and **F**) The impedance curve changed as (**E**) the proliferation and (**F**) the differentiation proceeded. (**G**) Impedance value measured at 17.7 kHz as the culture proceeded. Red and blue curves show the cells in growth and differentiation media, respectively. The control (black) used human dermal fibroblasts. (**H**) Conductance values calculated from IV curves with a range from −0.1 to +0.1 V. (**I**) Schematic illustration and TEM image (background image) of ROS-scavenging ceria nanoparticles. The ceria NPs are functionalized by oleylamine and methoxy-polyethylene glycol. (**J** and **K**) Fluorescence image of C2C12 myoblasts (stained with calcein AM) after 30 minutes of H_2O_2/Ceria NP treatment (**J**) and relative viability plot from fluorescence images (**K**). (**L**) Plots of impedance as a function of time in different treatment groups. Reproduced with permission from Kim SJ, Cho HR, Cho KW, et al. Multifunctional cell-culture platform for aligned cell sheet monitoring, transfer printing, and therapy. *ACS Nano*. 2015;9(3):2677–2688.[180] Copyright ©2015 American Chemical Society.

Abbreviations: ROS, reactive oxygen species; NP, nanoparticle; TEM, transmission electron microscope; PDMS, polydimethylsiloxane.

modified GO impacts other HRP inactivation pathways and hemotoxicity remains unknown. However, small lateral (*l*)-sized GO (200 nm) fragments are known to interact with DNA.[173] These interactions include DNA intercalation and the scission of DNA by GO/Cu^{2+} complexes. Furthermore, it has been shown that GO/Mn^{2+} and GO/Fe^{2+} complexes also cleave DNA. In addition, several investigations have shown that treatments of various cell lines with carbon nanomaterials such as rGO, graphene, and graphite can elevate the expression of p53, Rad 51, and MOGG1-1 reflecting chromosomal damage. Until recently, it was unclear whether DNA damage induced by graphene-based materials caused mutagenesis. In a recent study by Liu et al[174] GO treatments at concentrations of 10 and 100 µg/mL were found to alter gene expression in 101 genes involved in DNA-damage control, cell apoptosis, cell cycle, and metabolism. Intravenous injection of conventionally prepared GO at 4 mg/kg for 5 consecutive days induced formation of micronucleated polychromic erythrocytes in mice, and its mutagenesis potential appeared to be comparable with cyclophosphamide, a classic mutagen. However, traditionally prepared GO often contains high concentrations of Mn^{2+} (97 ppm) and Fe^{2+} WC. As stated previously, both metals are highly mutagenic in the presence of GO, nonspecific release of these ions from traditionally prepared GO might result in unusually high levels of toxicity and random scission of DNA. Consequently, researchers have started to use nontoxic oxidizing agents with greener exfoliating methods.[175] Of particular note is the recent work by Peng et al[176] in which an Fe^{2+}-based green strategy produced a single layer of GO in just 1 hour. Their approach resulted in the production of high purity GO containing 0.025 ppm of Mn^{2+} and 0.13 ppm Fe^{2+}, respectively. Results regarding the cytotoxicity of graphene-based nanomaterials remain conflicting (particular for GO). These discrepancies may be due to differences in the quality of the nanomaterials tested.[177,178]

Finally, there are many cautionary warnings in the literature[178] regarding the PEGlyated forms of GO and its ability to generate ROS in mammalian cells. However, ceria NPs are known to scavenge ROS and are therefore attractive candidates for inclusion into a graphene-based vehicles or TE platforms.[179] With this in mind, Kim et al[180] recently reported a graphene-based multifunctional platform that can suppress ROS generation. The multifunctional platform was capable of aligning plated cells and in situ monitoring of cellular physiological characteristics during proliferation and differentiation. Cell viability was represented by changes in impedance and monitored by an instrumented cell-culture platform (Figure 7). Treatment with 5 M H_2O_2 in differentiated C2C12 cells induced instant death in the majority of cells, resulting in a dramatic increase in impedance, whereas treatment with 5 mM H_2O_2 in the presence of ceria NPs yielded only minimal changes in impedance.

Conclusion

This review represents a snapshot of the current state of GO research and the opinions that govern its development. There is no doubt that GO has led to rapid improvements in many areas of biomedical science, including drug delivery, TE, sensors, imaging, and diagnosis within the last decade. Moreover, the recent advances in green fabrication methods[174] further extend the application potential of GO to a larger field of scientists. If this potential can then be coupled with the digitization and real-time monitoring of the cell sample (microdroplets), GO could be clinically exploited in the very near future. In our humble opinion, the great expectations fueling graphene-based research warrant a "digital shotgun" approach, thus clarifying any doubts regarding its efficacy and applicability not just in nanomedicine, but its future impact on environmental[181] and public health.

Acknowledgment

This research was supported by the National Research Foundation Korea project number 2012014335.

Disclosure

The authors report no conflicts of interest in this work.

References

1. Novoselov KS, Geim AK, Morozov SV, et al. Two-dimensional gas massless Dirac fermions in graphene. *Nature*. 2005;438(7065):197–200.
2. Lee C, Wei X, Kysar JW, Hone J. Measurement of the elastic properties and intrinsic strength of monolayer grapheme. *Science*. 2008; 321(5887):385–388.
3. Wang Y, Li Z, Wang J, Li J, Lin Y. Graphene and graphene oxide biofunctionlization and applications in biotechnology. *Trends Biotechnol*. 2011;29(5):205–212.
4. Liu Z, Robinson JT, Tabakman SM, Yang K, Dai H. Carbon materials for drug delivery and cancer therapy. *Mater Today*. 2011;14(7–8): 316–323.
5. Rao CNR, Sood AK, Subrahmanyam KS, Govindaraj A. Graphene the new two dimensional nanomaterial. *Angew Chem Int Ed Engl*. 2009;48(42):7752–7777.
6. Hummers WS, Offeman RE. Preparation of graphitic oxide. *J Am Chem Soc*. 1958;89(6):1339.
7. Dreyer DR, Park S, Bielawski CW, Ruoff R. The chemistry of graphene oxide. *Chem Soc Rev*. 2010;39(1):228–240.
8. Marcano DC, Kosynkin DV, Berlin JM, et al. Improved synthesis of graphene oxide. *ACS Nano*. 2010;4(8):4806–4814.
9. Fan H, Wang J, Wu H, et al. Fabrication, mechanical properties, and biocompatibility of graphene-reinforced chitosan composites. *Biomacromolecules*. 2010;11(9):2345–2351.
10. Ma J, Liu C, Li R, Wang J. Properties and structural characterization of oxide starch/chitosan/graphene oxide biodegradable nano-composites. *J Appl Polym Sci*. 2012;123(5):2933–2944.

11. Wojtoniszak M, Chen X, Kalenczuk RJ, Wajda A. Synthesis, dispersion, and cytocompatibility of graphene oxide and reduced graphene oxide. *Colloids Surf B Biointerfaces*. 2012;89(1):79–85.
12. Yang K, Wan J, Zhang S, Zhang Y, Lee S-T, Liu Z. In vivo pharmacokinetics, long-term biodistribution, and toxicology of PEGylated graphene in mice. *ACS Nano*. 2010;5(1):516–522.
13. Wang H, Qiu Z. Crystallization behaviors of biodegradable poly (l-lactic acid)/graphene oxide nano-composites from the amorphous states. *Thermochim Acta*. 2011;526(1–2):229–236.
14. Wan C, Chen B. Poly(ε-caprolactone)/graphene oxide biocomposites: mechanical properties and bioactivity. *Biomed Mater*. 2011;6(5): 055010.
15. Zhang J, Qiu Z. Morphology, crystallization behavior, and dynamic mechanical properties of biodegradable poly(ε-caprolactone)/thermally reduced graphene nanocomposites. *Ind Eng Chem Res*. 2011;50(24): 13885–13891.
16. Liu JQ, Cui L, Dusan L. Graphene and graphene oxide as new nanocarriers for drug delivery applications. *Acta Biomater*. 2013;9(12):9243–9257.
17. Feng L, Wu L, Qu X. New horizons for diagnostics and therapeutic applications of graphene and graphene oxide. *Adv Mater*. 2013; 25(2):168–186.
18. Pan Y, Sahoo NG, Li L. The application of graphene oxide in drug delivery. *Expert Opin Drug Deliv*. 2012;12(9):1365–1376.
19. Shen H, Zhang L, Liu M, Zhang Z. Biomedical applications of graphene. *Theranostics*. 2012;2(3):283–294.
20. Chen Y, Tan C, Zhang H, Wang L. Two dimensional graphene analogues for biomedical applications. *Chem Soc Rev*. 2015;44(9):2681–2701.
21. Chen BA, Liu M, Zhang LM, Huang J, Yao JL, Zhang ZJ. Polyethylenimine-functionalized graphene oxide as an efficient gene delivery vector. *J Mater Chem*. 2011;21:7736–7741.
22. Rana VK, Choi MC, Kong JY, et al. Synthesis and drug-delivery behavior of chitosan functionalized graphene oxide hybrid nanosheets. *Macromol Mater Eng*. 2011;296(2):131–140.
23. Kakran NGSM, Bao H, Pan Y, Li L. Functionalized graphene oxide as nanocarrier for loading and delivery of ellagic acid. *Curr Med Chem*. 2011;18(19):4503–4512.
24. Liu K, Zhang JJ, Cheng FF, Zheng TT, Wang C, Zhu JJ. Green and facile synthesis of highly biocompatible graphene nanosheets and its application for cellular imaging and drug delivery. *J Mater Chem*. 2011; 21(32):12034–12040.
25. Liu Z, Robinson JT, Sun X, Dai H. PEGylated nanographene oxide for delivery of water-insoluble cancer drugs. *J Am Chem Soc*. 2008;130(33):10876–10877.
26. Kim MG, Park JY, Miao W, Lee J, Oh YK. Polyaptamer DNA nanothread-anchored, reduced graphene oxide nanosheets for targeted delivery. *Biomaterials*. 2015;48:129–136.
27. Zhang L, Xia J, Zhao Q, Liu L, Zhang Z. Functional graphene oxide as a nanocarrier for controlled loading and targeted delivery of mixed anticancer drugs. *Small*. 2010;6(4):537–544.
28. Wen H, Dong C, Dong H, et al. Engineered redox-responsive peg detachment mechanism in pegylated nano-graphene oxide for intracellular drug delivery. *Small*. 2012;8(5):760–769.
29. Mudavath SL, Talat M, Rai M, Srivastava ON, Sundar S. Characterisation and evaluation of amine modified graphene amphotericin B for the treatment of visceral leishmaniasis: in vivo and in vitro studies. *Drug Des Devel Ther*. 2014;8:1235–1247.
30. Prajapati VK, Awasthi K, Yadav TP, Rai M, Srivastava ON, Sundar S. An oral formulation of amphotericin B attached to functionalized carbon nanotube is an effective treatement for experimental visceral leishmaniasis. *J Infect Dis*. 2012;205(2):333–336.
31. Wang Y, Wang H, Liu D, Song S, Wang X, Zhang H. Graphene oxide covalently grafted upconversion nanoparticles for combined NIR mediated imaging and photothermal/photodynamic cancer therapy. *Biomaterials*. 2013;34(31):7715–7724.
32. Lee WC, Lim CHYX, Shi H, et al. Origin of enhanced stem cell growth and differentiation on graphene and graphene oxide. *ACS Nano*. 2011;5(9):7334–7341.
33. Kim TK, Shah S, Yang L. Controlling differentiation of adipose-derived stem cells using combinatorial graphene hybrid-pattern arrays. *ACS Nano*. 2015:9(4):3780–3790.
34. Tang LA, Lee WC, Shi H, et al. Highly wrinkled cross-linked graphene oxide membranes for biological and charge-storage applications. *Small*. 2012;8(3):423–431.
35. La WG, Jin M, Park S, Yoon HH, Jeong GJ, et al. Delivery of bone morphogenetic protein-2 and substance P using graphene oxide for bone regeneration. *Int J Nanomedicine*. 2014;9(1):107–116.
36. Lim HN, Huang NM, Lim SS, Harrison I, Chia CH. Fabrication and characterization of graphene hydrogel via hydrothermal approach as a scaffold for preliminary study of cell growth. *Int J Nanomedicine*. 2011;6:1817–1823.
37. Shin SR, Aghaei-Ghareh-Bolagh B, Gao X, Nikkhah M, Jung SM, et al. Layer-by-layer assembly of 3d tissue constructs with functionalized graphene. *Adv Funct Mater*. 2014;24(39):6136–6144.
38. Chaudhuri B, Bhadra D, Moroni L, Pramanik K. Myoblast differentiation of human mesenchymal stem cells on graphene oxide and electrospun graphene oxide–polymer composite fibrous meshes: importance of graphene oxide conductivity and dielectric constant on their biocompatibility. *Biofabrication*. 2015;7(1):015009.
39. Gurunathan S, Han JW, Dayem AA, Eppakayla V, Kim JH. Oxidative stress-mediated antibacterial activity of graphene oxide and reduced graphene oxide in *Pseudomonas aeruginosa*. *Int J Nanomedicine*. 2012; 7:5901–5914.
40. Nanda SS, An SSA, Yi. Oxidative stress and antibacterial properties of a graphene oxide-cystamine nanohybrid. *Int J Nanomedicine*. 2015; 10:549–556.
41. Kurantowicz N, Sawosz E, Jaworsk S, et al. Interaction of graphene family materials with Listeria monocytogenes and Salmonella enterica. *Nanoscale Res Lett*. 2015;10(23). doi:10.1186/s11671-015-0749-y.
42. Chen H, Gao D, Wang B, et al. Graphene oxide as an anaerobic membrane scaffold and antagonistic effects against pathogenic *E. coli* and *S. aureus*. *Nanotechnology*. 2014;25(16):165101.
43. Zhan S, Zhu D, Ma S, et al. Highly efficient removal of pathogenic bacteria with magnetic graphene composite. *ACS Appl Mater Interfaces*. 2015;7(7):4290–4298.
44. Mangadlao JD, Santos CM, Felipe MJL, Leon ACC, Rodrigues DF, Advincula RC. On the antibacterial mechanism of graphene oxide (GO) Langmuir–Blodgett films. *Chem Commun*. 2015;51(14): 2886–2889.
45. Liu S, Zeng TH, Hofmann M, et al. Antibacterial activity of graphite, graphite oxide, graphene oxide, and reduced graphene oxide: membrane and oxidative stress. *ACS Nano*. 2011;5(9):6971–6980.
46. Hu W, Peng C, Luo W, et al. Graphene-based antibacterial paper. *ACS Nano*. 2010;4(7):4317–4323.
47. Gurunathan S, Han JW, Dayem AA, et al. Antibacterial activity of dithiothreitol reduced graphene oxide. *J Ind Eng Chem*. 2013;19(4): 1280–1288.
48. Mogharabi M, Abdollahi M, Faramarzi MA. Safety concerns to application of graphene compounds in pharmacy and medicine. *J Pharm Sci*. 2014;22(1). doi:10.1186/2008-2231-22-23.
49. Nguyen P, Berry V. Graphene interfaced with biological cells: opportunities and challenges. *J Phys Chem Lett*. 2012;3(8):1024–1029.
50. Mejias Carpio IE, Santos CM, Wei X, Rodrigues DF. Toxicity of a polymer–graphene oxide composite against bacterial planktonic cells, biofilms, and mammalian cells. *Nanoscale*. 2012;4(15):4746–4756.
51. Sreeprasad TS, Maliyekkal MS, Deepti K, Chaudhari K, Xavier PL, Pradeep T. Transparent, luminescent, antibacterial and patternable film forming composites of graphene oxide/reduced graphene oxide. *ACS Appl Mater Interfaces*. 2011;3(7):2643–2654.
52. Huang N, Liu M, Li M, Zhang Y, Yao S. Synergetic signal amplification based on electrochemical reduced graphene oxide-ferrocene derivative hybrid and gold nanoparticles as an ultrasensitive detection platform for bisphenol A. *Anal Chim Acta*. 2015;853:249–257.
53. Gao L, Lian C, Zhou Y, et al. Graphene oxide-DNA based sensors. *Biosens Bioelectron*. 2014;60:22–29.

54. Zhang B, Li Q, Cui T. Ultrasensitive suspended nanocomposite cancer sensors with strong suppression of electrical noise. *Biosens Bioelectron*. 2012;31(1):105–109.
55. Gu Y, Ju C, Li Y, et al. Detection of circulating tumor cell in prostate cancer based on carboylated graphene oxide modified light addressable potentiometric sensor. *Biosens Bioelectron*. 2015;66:24–31.
56. Yao Y, Xue Y. Impedance analysis of quartz crystal microbalance humidity sensors based on nanodiamond/graphene oxide nanocomposite film. *Sens Actuators B Chem*. 2015;211:52–58.
57. Ge S, Sun M, Liu W, et al. Disposable electrochemical immune-sensors based on peroxidase-like magnetic silica graphene composites for detection of cancer antigen 153. *Sens Actuators B Chem*. 2014;192:317–326.
58. Jaque D, Martinez Maestro L, del Rosal B, et al. Nanoparticles for photothermal therapies. *Nanoscale*. 2014;6(16):9494–9530.
59. Johannsen M, Gneveckow U, Eckelt L, et al. Clinical hyperthermia of prostate cancer using magnetic nanoparticles: presentation of a new interstitial technique. *Int J Hyperthermia*. 2005;21(7):637–647.
60. Lim DK, Barhoumi A, Wylie RG, et al. Enhanced photothermal effect of plasmonic nanoparticles coated with reduced graphene oxide. *Nano Lett*. 2013;13(9):4075–4079.
61. Huschka R, Zuloaga J, Knight MW, Brown LV, Nordlander P, Halas NJ. Light-induced release of DNA from gold nanoparticles: nanoshells and nanorods. *J Am Chem Soc*. 2011;133(31):12247–12255.
62. Shi X, Gong H, Li Y, Wang C, Cheng L, Liu Z. Graphene-based magnetic plasmonic nanocomposite for dual bioimaging and photothermal therapy. *Biomaterials*. 2013;34(20):4786–4793.
63. Huang J, Zhang LM, Chen BA. Nanocomposites of size-controlled gold nanoparticles and graphene oxide: Formation and applications in SERS and catalysis. *Nanoscale*. 2010;2(12):2733–2738.
64. Liu Q, Wei L, Wang J, et al. Cell imaging by graphene oxide based on surface enhanced Raman scattering. *Nanoscale*. 2012;4(22):7084–7089.
65. Huang J, Zong C, Shen H, et al. Mechanism of cellular uptake of graphene oxide studied by surface-enhanced Raman spectroscopy. *Small*. 2012;8(16):2577–2584.
66. Liu ZM, Guo ZY, Zhong HQ, Qin XC, Wan MM, Yang BW. Graphene oxide based surface-enhanced Raman scattering probes for cancer cell imaging. *Phys Chem Chem Phys*. 2013;15(8):2961–2966.
67. Weitman SD, Lark RH, Coney LR, et al. Distribution of the folate receptor GP38 in normal and malignant cell lines and tissues. *Cancer Res*. 1992;52(12):3396–3401.
68. Zwicke GL, Mansoori GA, Jeffery CJ. Utilizing the folate receptor for active targeting of cancer nanotherapeutics. *Nano Rev*. 2012;3. doi:org/10.3402/nano.v3i0.18496.
69. Gurunathan S, Han JW, Eppakayla V, Kim JH. Green synthesis of graphene and its cytotoxic effects in human breast cancer cells. *Int J Nanomedicine*. 2013;8:1015–1027.
70. Hinzmann M, Jaworski S, Kutwin M, et al. Nanoparticles containing allotropes of carbon have genotoxic effects on glioblastoma multiforme cells. *Int J Nanomedicine*. 2013;9:2409–2417.
71. Wang H, Gu W, Xiao N, Ye L, Xu Q. Chlorotoxin-conjugated graphene oxide for targeted delivery of an anticancer drug. *Int J Nanomedicine*. 2014;9:1433–1442.
72. Chowdhury SM, Surhland C, Sanchez Z, et al. Graphene nanoribbons as a drug delivery agent for lucanthone mediated therapy of glioblastoma multiforme. *J Nanomed Nanotechnol*. 2015;11(1):109–118.
73. Shen H, Zhang L, Liu M, et al. Biomedical applications of graphene. *Theranostics*. 2012;2(3):283–294.
74. Shi S, Yang K, Hong H, et al. Tumor vasculature targeting and imaging in living mice with reduced graphene oxide. *Biomaterials*. 2013;34(12):3002–3009.
75. Qin XC, Guo ZY, Liu ZM, et al. Folic acid-conjugated graphene oxide for cancer targeted chemo-photothermal therapy. *J Photochem Photobiol B*. 2013;120:156–162.
76. Bussy C, Boucetta A, Kostarelos K. Safety considerations for graphene: Lessons learnt from carbon nanotubes. *Acc Chem Res*. 2013;46(3):692–701.
77. Dallavelle M, Calvaresi M, Bottoni A, Franco MM, Zerbetto F. Graphene can wreak havoc with cell membranes. *ACS Appl Mater Interfaces*. 2015;7(7):4406–4414.
78. Liu J, Cui L, Losic D. Graphene and graphene oxide as new nanocarriers for drug delivery applications. *Acta Biomater*. 2013;9(12):9243–9257.
79. Smolkova B, Yamani NE, Collins AR, Gutleb AC, Dusinska M. Nanoparticles in food. Epigenetic changes induced by nanomaterials and possible impact on health. *Food Chem Toxicol*. 2015;77:64–73.
80. Georgantzopoulou A. *Effects of Silver Nanoparticles and Ions and Interaction with the First Line of Defense*. [PhD]. Wageningen: Wageningen University; 2015:188 p.
81. Nilsson EE, Skinner MK. Environmentally induced epigenetic transgenerational inheritance of disease susceptibility. *Transl Res*. 2014;165(1):12–17.
82. Dubey P, Matai I, Kumar SU, Sachdev A, Bhushan B, Gopinath P. Perturbation of cellular mechanistic system by silver nanoparticles toxicity: cytotoxic, genotoxic and epigenetic potential. *Adv Colloid Interface Sci*. 2015;221:4–21.
83. Yao Y, Costa M. Genetic and epigenetic effects of nanomaterials. *J Mol Genet Med*. 2013;7(4). doi:10.4172/1747-0862.1000086.
84. Ahluwalia A, Boraschi D, Byrne HJ, et al. The bio-nano interface as a basis for predicting nanoparticle fate and behavior in living organisms: towards grouping and catergorizing of nanomaterials and nanosafety by design. *Bio Nano Materials*. 2013;14:195–216.
85. Seabra AB, Paula AJ, Lima R, Alves OL, Duran N. Nanotoxicity of graphene and graphene oxide. *Chem Res Toxicol*. 2014;27(2):159–168.
86. Servant A, Bianco A, Prato M, Kostarelos K. Graphene for multifunctional synthetic biology: the last 'zeitgeist' in nanomedicine. *Bioorg Med Chem Lett*. 2014;24(7):1638–1649.
87. Shi S, Chen F, Ehlerding EB, Cai W. Surface engineering of graphene based nanomaterials for biomedical applications. *Bioconjug Chem*. 2014;25(9):1609–1619.
88. Goenka S, Sant V, Sant S. Graphene-based nanomaterials for drug delivery and tissue engineering. *J Control Release*. 2014;173:75–88.
89. Zhang H, Gruner G, Zhao Y. Recent advancements of graphene in biomedicine. *J Mater Chem B Mater Biol Med*. 2013;1(20):2542–2567.
90. Soenen SJ, Parak WJ, Reijman J, Manshian B. (Intra) Cellular stability of inorganic nanoparticles: effects on cytotoxicity, particle functionality, and biomedical application. *Chem Rev*. 2015;115(5):2109–2135.
91. Parveen S, Misra R, Sahoo SK. Nanoparticles: a boon to drug delivery, therapeutics, diagnostics and imaging. *J Nanomed Nanotechnol*. 2012;8(2):147–66.
92. Yang K, Zhang SA, Zhang GX, Sun XM, Lee ST, Liu ZA. Graphene in mice:ultrahigh in vivo tumor uptake and efficient photothermal therapy. *Nano Lett*. 2010;10(9):3318–3323.
93. Sun XM, Liu Z, Welsher K, et al. Nanographene oxide for cellular imaging and drug delivery. *Nano Res*. 2008;1(3):203–212.
94. Ali Boucetta H, Bitounis D, Raveendran-Nair R, Servant A, Van den Bossche J, Kostarelos K. Purified graphene oxide dispersions lack in vitro cytotoxicity and in vivo pathogenicity. *Adv Healthc Mater*. 2013;2(3):433–441.
95. Dinauer N, Balthasar S, Weber C, Kreuter J, Langer K, von Briesen H. Selective targeting of antibody-conjugated nanoparticles to leukemic cells and primary T-lymphocytes. *Biomaterials*. 2005;26(29):5898–906.
96. Nasongkla N, Shuai X, Ai H, et al. CRGD functionalized polymer micelles for targeted doxorubicin delivery. *Angew Chem Int Ed Engl*. 2004;116(46):6483–6487.
97. Daniels TR, Delgado T, Helguera G, Penichet ML. The transferrin receptor part II: targeted delivery of therapeutic agents into cancer cells. *Clin Immunol*. 2006;121(2):159–176.
98. Yang XY, Zhang XY, Liu ZF, Ma YF, Huang Y, Chen Y. High-efficiency loading and controlled release of doxorubicin hydrochloride on graphene oxide. *J Phys Chem C Nanomater Interfaces*. 2008;112(45):17554–17558.
99. Depan D, Shah J, Misra RDK. Controlled release of drug from folate-decorated and graphene mediated drug delivery system: synthesis, loading efficiency, and drug release response. *Mater Sci Eng C Mater Biol Appl*. 2011;31(7):1305–1312.
100. Mendes RG, Bachmatiuk A, Büchner B, Cuniberti G, Rümmeli MH. Carbon nanostructures as multi-functional drug delivery platforms. *J Mater Chem B Mater Biol Med*. 2013;1(4):401–428.

101. Zhang YB, Ali SF, Dervishi E, et al. Cytotoxicity effects of graphene and single-wall carbon nanotubes in neural phaeochromocytoma-derived PC12 cells. *ACS Nano*. 2010;4(6):3181–3186.
102. Bai H, Li C, Wang XL, Shi GQ. A pH-sensitive graphene oxide composite hydrogel. *Chem Commun*. 2010;46(14):2376–2378.
103. Zhao X, Yang L, Li X, et al. Functionalized graphen oxide nanoparticles for cancer cell specific delivery of antitumor drug. *Bioconjug Chem*. 2015;26(1):128–136.
104. Lu YJ, Yang HW, Hung SC, et al. Improving thermal stability and efficacy of BCNU in treating glioma cells using PAA functionalized graphene oxide. *Int J Nanomedicine*. 2012;7:1737–1747.
105. Xiong H, Guo Z, Zhang W, Zhong H, Liu S, Ji Y. Redox-responsive biodegradable PEGylated nanographene oxide for efficiently chemo-photothermal therapy: a comparative study with non-biodegradable PEGylated nanographene oxide. *J Photochem Photobiol B*. 2014;138:191–201.
106. Zhou K, Zhu Y, Yang X, Li C. One-pot preparation of graphene/Fe_3O_4 composites by a solvothermal reaction. *New J Chem*. 2010;34(12):2950–2955.
107. Liu HW, Hu SH, Chen YW, Chen SY. Characterization and drug release behavior of highly responsive chip-like electrically modulated reduced graphene oxide poly(vinyl alcohol) membranes. *J Mater Chem*. 2012;22(33):17311–17320.
108. Servant A, Leon V, Jasim D, et al. Graphene-based electroresponsive scaffolds as polymeric implants for on-demand drug delivery. *Adv Healthc Mater*. 2014;3(8):1334–1343.
109. Wang H, Gu W, Xiao N, Ye L, Xu Q. Chlorotoxin-conjugated graphene oxide for targeted delivery of an anticancer drug. *Int J Nanomedicine*. 2014;9:1433–1442.
110. Yang K, Feng L, Liu Z. The advancing uses of nano-graphene in drug delivery. *Expert Opin Drug Deliv*. 2015;12(4):601–612.
111. Kim TH, Lee GJ, Kang JH, Kim HJ, Kim T, Oh JM. Anticancer drug-incorporated layered double hydroxide nanohybrids and their enhanced anticancer therapeutic efficacy in combination cancer treatment. *Biomed Res Int*. 2014;2014:193401. doi:10.1155/2014/193401.
112. Balcioglu M, Buyukbekar BZ, Yavuz MS, Yigit MV. Smart-polymer-functionalized graphene nanodevices for thermo-switch-controlled biodetection. *ACS Biomater Sci Eng*. 2015;1(1):27–36.
113. Zhi F, Dong H, Jia X, et al. Functionalized graphene oxide mediated adriamycin delivery and miR-21 gene silencing to overcome tumor multidrug resistance in vitro. *Plos One*. 2013;8(3):e60034.
114. Feng L, Zhang S, Liu Z. Graphene based gene transfection. *Nanoscale*. 2011;3(3):1252–1257.
115. El-Aneed A. An overview of current delivery systems in cancer gene therapy. *J Control Release*. 2004;94(1):1–14.
116. Li Y, Ren T, Li L, Cai X, Dong H, Liu S. Engineered polyethylenimine/graphene oxide nanocomposite for nuclear localized gene delivery. *Polym Chem*. 2012;3(9):2561–2569.
117. Whitehead KA, Langer R, Anderson DG. Knocking down barriers: advances in siRNA delivery. *Nat Rev Drug Discov*. 2009;8(2):129–138.
118. Zhang LM, Lu ZX, Zhao QH, Huang J, Shen H, Zhang ZJ. Enhanced chemotherapy efficacy by sequential delivery of siRNA and anticancer drugs using PEI-grafted graphene oxide. *Small*. 2011;7(4):460–464.
119. Li K, Feng L, Shen J, et al. Patterned substrates of nano-graphene oxide mediating highly localized and efficient gene delivery. *ACS Appl Mater Interfaces*. 2014;5(8):5900–5907.
120. Tripathi SK, Goyal R, Gupta KC, Kumar P. Functionalized graphene oxide mediated nucleic acid delivery. *Carbon*. 2013;51:224–235.
121. Bao HQ, Pan YZ, Ping Y, et al. Chitosan-functionalized graphene oxide as nanocarriers for drug and gene delivery. *Small*. 2011;7(11):1569–1578.
122. Zhang LM, Wang ZL, Lu ZX, et al. PEGylated reduced graphene oxide as a superior ssRNA delivery system. *J Mater Chem B Mater Biol Med*. 2013;1(6):749–755.
123. Liu X, Ma D, Tang H, et al. Polyamidoamine dendrimer and oleic acid-functionalized graphene as biocompatible and efficient gene delivery vectors. *ACS Appl Mater Interfaces*. 2014;6(11):8173–8183.
124. Tian B, Wang C, Zhang S, Feng L, Liu Z. Photo-thermally enhanced photodynamic therapy delivered by nano-graphene oxide. *ACS Nano*. 2011;5(9):7000–7009.
125. Kim H, Lee D, Kim J, Kim T, Kim WJ. Photo-thermally triggered cytosolic drug delivery via endosome disruption using a functionalized reduced graphene oxide. *ACS Nano*. 2013;7(8):6735–6746.
126. Kim H, Kim WJ. Photothermally controlled gene delivery by reduced graphene oxide-polyethylenimine nanocomposite. *Small*. 2014;10(1):117–126.
127. Gautschi OP, Frey SP, Zellweger R. Bone morphogentic proteins in clinical applications. *ANZ J Surg*. 2007;77(8):626–631.
128. Termaat MF, Den Boer FC, Bakker FC, Patka P, Haarman HJ. Bone morphogenetic genetic proteins. Development and clinical efficacy in the treatment of fractures and bone defects. *J Bone Joint Surg Am*. 2005;87(6):1367–1378.
129. Govender S, Csimma C, Genant HK, et al; BMP-2 Evaluation in Surgery for Tibial Trauma (BESTT) Study Group. Recombinant human bone morphogenetic protein-2 for treatment of open tibial fractures: a prospeactive, controlled, randomized study of four hundred and fifty patients. *J Bone Joint Surg Am*. 2002;84A(12):2123–2134.
130. Madeira C, Santhagunam A, Salgueiro JB, Cabral JMS. Advanced cell therapies for articular cartilage regeneration. *Trends Biotechnol*. 2015;33(1):35–42.
131. Campbell S, Maitland D, Hoare T. Enhanced pulsatile drug release from injectable magnetic hydrogels with embedded thermosensitive microgels. *ACS Macro Lett*. 2015;4(3):312–316.
132. Matsusaki M, Ajiro H, Kida T, Serizawa T, Akashi M. Layer-by-layer assembly through weak interactions and their biomedical applications. *Adv Mater*. 2012;24(4):454–474.
133. Nishiguchi A, Yoshida H, Matsusaki M, Akashi M. Rapid. Construction of three-dimensional multilayered tissues with endothelial tube networks by the cell-accumulation technique. *Adv Mater*. 2011;23(31):3506–3510.
134. Justin R, Chen B. Body temperature reduction of graphene oxide through chitosan functionalisation and its application in drug delivery. *Mater Sci Eng C Mater Biol Appl*. 2014;34:50–53.
135. Shin SR, Aghaei-Ghareh-Bolagh B, Gao X, et al. Layer-by-layer assembly of 3D tissue constructs with functionalized graphene. *Adv Mater*. 2014;22(39):6136–6144.
136. Zhou H, Cheng C, Qin H, et al. Self-assembled 3D compatible and bioactive layer at the macro-interface via graphene based supermolecules. *Polym Chem*. 2014;5(11):3563–3575.
137. Qi W, Xue Z, Yuan W, Wang H. Layer-bylayer assembled graphene oxide composite films for enhanced mechanical properties and fibroblast cell affinity. *J Mater Chem B Mater Biol Med*. 2014;2(3):325–331.
138. Wang L, Chunxiang L, Zhang B, Zhao B, Wu F, Guan S. Fabrication and characterization of flexible silk fibroin films reinforced with graphene oxide for biomedical applications. *RSC Adv*. 2014;4(76):40312–40320.
139. Deepachitra R. Nigam R, Prohit SD, et al. In vitro study of hydroxyapatite coatings on fibrin functionalized/pristine graphene oxide for bone grafting. *Mater Manuf Process*. 2014;30(6):804–811.
140. Ryu S, Kim B. Culture of neural cells and stem cells on graphene. *J Tissue Eng Regen Med*. 2013;10(2):39–46.
141. Hong SW, Lee JH, Kang SH, et al. Enhanced neural cell adhesion and neurite outgrowth on graphene-based biomimetric substrates. *Biomed Res Int*. 2014. doi/10.1155/2014/21249.
142. Kim T, Shah S, Yang L, et al. Controlling differentiation of adipose-derived stem cells using combinatorial graphene hybrid-pattern arrays. *ACS Nano*. 2015;9(4):3780–3790.
143. Bressan E, Ferroni L, Gardin C, et al. Graphene based scaffolds effects on stem cells commitment. *J Transl Med*. 2014;12:296–310.
144. Sreejith S, Ma X, Zhao Y. Graphene oxide wrapping on squaraine-loaded mesoporous silica nanoparticles for bioimaging. *J Am Chem Soc*. 2012;134(42):17346–17349.
145. Ananta JS, Godin B, Sethi R, et al. Geometrical confinement of gadolinium-based contrast agents in nanoporous particles enhances T1 contrast. *Nat Nanotechnol*. 2010;5(11):815–821.

146. Kanakia S, Toussaint JD, Chowdury SM, et al. Physicochemical characterization of a novel graphene-based magnetic resonance imaging contrast agent. *Int J Nanomedicine*. 2013;8:2821–2833.
147. Gollavelli G, Ling YC. Multifunctional graphene as an *in-vitro* and *in-vivo* imaging probe. *Biomaterials*. 2012;33(8):2532–2545.
148. Zhang H, Wu H, Wang J, et al. Graphene oxide-$BaGdF_5$ nanocomposites for multi-modal imaging and photothermal therapy. *Biomaterials*. 2015;42:66–77.
149. Hong H, Zhang Y, Engle JW, et al. In vivo targeting and positron emission tomography imaging of tumor vasculature with ^{66}Ga-labeled nano-graphene. *Biomaterials*. 2012;33(16):4147–4156.
150. Srivastava S, Awasthi R, Tripathi D, et al. Magnetic-nanoparticle-doped carbogenic nanocomposite: an effective magnetic resonance/fluorescence multimodal imaging probe. *Small*. 2012;8(7):1099–1109.
151. Cianfrocca M, ScD SL, Roenn JV. Randomized trial of paclitaxel versus pegylated liposomal doxorubicin for advanced human immunodeficiency virus-associated Kaposi sarcoma. *Cancer*. 2010;116(16):3969–3977.
152. Josefsen LB, Boyle RW. Unique diagnostic and therapeutic roles of porphyrins and phthalocyanines in photodynamic therapy, imaging and theranostics. *Theranostics*. 2012;2(9):916–966.
153. Agostinis P, Berg K, Cengel KA, et al. Photodynamic therapy of cancer: an update. *CA Cancer J Clin*. 2011;61:250–281.
154. Yang K, Wan J, Zhang S, Tian B, Zhang Y, Liu Z. The influence of surface chemistry and particle size of nanoscale graphene oxide on photothermal therapy of cancer using ultra-low laser power. *Biomaterials*. 2012;33(7):2206–2214.
155. Zheng X, Morgan J, Pandey SK, et al. Conjugation of 2′-(1′-hexyloxyethyl)-2-devinylpyropheophorbide-a (HPPH) to carbohydrates changes its subcellular distribution and enhances photodynamic activity in vivo. *J Med Chem*. 2009;52(14):4306–4318.
156. Ethirajan M, Chen YH, Joshi P, Pandey RK. The role of porphyrin chemistry in tumor imaging and photodynamic therapy. *Chem Soc Rev*. 2011;40(1):340–362.
157. Srivatsan A, Ethirajan M, Pandey SK, et al. Conjugation of cRGD peptide to chlorophyll a based photosensitizer (HPPH) alters its pharmacokinetics with enhanced tumor-imaging and photosensitizing (PDT) efficacy. *Mol Pharm*. 2011;8(4):1186–1197.
158. Rong P, Yang K, Srivastan A, et al. Photosensitizer loaded nano-graphene for multimodal imaging guided tumor photodynamic therapy. *Theranostics*. 2014;4(3):229–239.
159. Chen H, Hwang JH. Ultrasound-targeted microbubble destruction for chemotherapeutic drug delivery to solid tumors. *J Ther Ultrasound*. 2013;1:10. doi:10.1186/2050-5736-1-10.
160. Li JL, Hou XL, Bao HC, et al. Graphene oxide nanoparticles for enhanced photothermal cancer cell therapy under the irradiation of a femtosecond laser beam. *J Biomed Mater Res A*. 2014;102(7):2181–2188.
161. Chen D, Dougherty CA, Zhu K, Hong H. Theranostic applications of carbon nanomaterials in cancer: focus on imaging and cargo delivery. *J Control Release*. 2015;210:230–245.
162. Feng L, Liu Z. Graphene in biomedicine: opportunities and challenges. *Nanomedicine*. 2011;6(2):317–324.
163. Robinson JT, Tabakman SM, Liang Y, et al. Ultrasmall reduced graphene oxide with high near-infrared absorbance for photothermal therapy. *J Am Chem Soc*. 2011;133(17):6825–6831.
164. Chang Y, Yang ST, Liu JH, et al. In vitro toxicity evaluation of graphene oxide on A549 cells. *Toxicol Lett*. 2011;200(3):201–210.
165. Yue H, Wei W, Yue Z, et al. The role of the lateral dimension of graphene oxide in the regulation of cellular responses. *Biomaterials*. 2012;33(16):4013–4021.
166. Mu Q, Su G, Li L, et al. Size-dependent cell uptake of protein-coated graphene oxide nanosheets. *ACS Appl Mater Interfaces*. 2012;4(4):2259–2266.
167. Sasidharan A, Panchakarla LS, Sadanandan AR, et al. Hemocompatibility and macrophage response of pristine and functionalized graphene. *Small*. 2012;8(8):1251−1263.
168. Liao KH, Lin YS, Macosko CW, Haynes CL. Cytotoxicity of graphene oxide and graphene in human erythrocytes and skin fibroblasts. *ACS Appl Mater Interfaces*. 2011;3(7):2607−2615.
169. Ding Z, Zhang Z, Ma H, Chen Y. In vitro hemocompatibility and toxic mechanism of graphene oxide on human peripheral blood T lymphocytes and serum albumin. *ACS Appl Mater Interfaces*. 2014;6(22):19797−19807.
170. Mao L, Luo S, Huang Q, Lu J. Horseradish peroxidase inactivation heme destruction and influence of polyethylene glycol. *Sci Rep*. 2013;3:3126. doi:10.1038/srep03126.
171. Bai H, Jiang W, Kotchey GP, et al. Insight into the mechanism of graphene oxide degradation via the photo-fenton reaction. *J Phys Chem C Nanomater Interfaces*. 2014;118(19):10519–10529.
172. Zhu L, Chang DW, Dai L, Hong Y. DNA damage induced by multiwalled carbon nanotubes in mouse embryonic stem cell. *Nano Lett*. 2007;7(12):3592–2597.
173. Ren H, Wang C, Zhang J. DNA cleavage system of nanosized graphene oxide sheets and copper ions. *ACS Nano*. 2010;4(12):7169–7174.
174. Liu Y, Luo Y, Wu J, et al. Graphene oxide can induce *in vitro* and *in vivo* mutagenesis. *Sci Rep*. 2013;3. doi:10.1038/srep03469.
175. Gurunathan S, Han JW, Kim JH. Green chemistry approach for the synthesis of biocompatible graphene. *Int J Nanomedicine*. 2013;8:2719–2732.
176. Peng L, Xu Z, Liu Z, et al. An iron-based green approach to 1-h production of single layer graphene oxide. *Nat Commun*. 2015;6:5716. doi:10.1038/ncomms6716.
177. Nezakati T, Cousins BG, Seifalian AM. Toxicology of chemically modified graphene-based materials for medical application. *Arch Toxicol*. 2014;88(11):1987–2012.
178. Yin PT, Shah S, Chhowalla M, Lee KB. Design, synthesis, and characterization of graphene-nanoparticle hybrid materials for bioapplications. *Chem Rev*. 2015;115(7):2483–2531.
179. Karakoti A, Singh S, Dowding JM, Seal S, Self WT. Redox-active radical scavenging nanomaterials. *Chem Soc Rev*. 2010;39(11):4422–4432.
180. Kim SJ, Cho HR, Cho KW, et al. Multifunctional cell-culture platform for aligned cell sheet monitoring, transfer printing, and therapy. *ACS Nano*. 2015;9(3):2677–2688.
181. Hou WC, Chowdhury I, Goodwin DG, et al. Photochemical transformation of graphene oxide in sunlight. *Environ Sci Technol*. 2015;49(6):3435–3443.